







# Impact of Snowfall on Terahertz Channel Performance: Measurement and Modeling Insights

Guohao Liu, Xiangkun He , Jiabiao Zhao, Da Li , Hong Liang , Houjun Sun ,  
Daniel M. Mittleman , *Fellow, IEEE*, and Jianjun Ma , *Member, IEEE*

**Abstract**—In the evolving domain of wireless communication, the investigation of the terahertz (THz) frequency spectrum, spanning 0.1–10 THz, has become a critical focus for advancing ultra-high-speed data transmission technologies. The effective deployment of THz wireless communication techniques mandates a complete study of channel performance under various atmospheric conditions, such as rain, fog, cloud, haze, and, notably snow. These environmental elements significantly impact the design of the protocol stack, ranging from physical-layer signal processing to application design and strategic network planning. An in-depth understanding of channel propagation and fading characteristics in real-world environments, especially over ultrawide bandwidths, is crucial. This work presents a comprehensive measurement-based and theoretical investigation of Line-of-Sight (LoS) THz channel performance in snowy conditions. It methodically examines both the empirical and predicted aspects of channel power and bit-error-ratio (BER). The effects of snowfall rate, carrier frequency, ambient temperature, and relative humidity on channel performance are analyzed and discussed. Our findings demonstrate that snowy conditions not only exert power loss but also induce rapid fluctuations in the power levels of the THz channel. Notably, our results reveal an absence of significant multipath effects in these scenarios. This insight highlights the need for further research into the dynamics of snowflake movement and their interaction with THz transmission paths.

**Index Terms**—Bit-error-ratio (BER), power loss, snowy weather, terahertz (THz) wireless channel.

Manuscript received 5 February 2024; revised 20 March 2024 and 30 April 2024; accepted 3 June 2024. Date of publication 21 June 2024; date of current version 5 September 2024. This work was supported in part by the National Natural Science Foundation of China under Grant 62071046, in part by the Science and Technology Innovation Program of Beijing Institute of Technology under Grant 2022CX01023, in part by the Talent Support Program of Beijing Institute of Technology “Special Young Scholars” under Grant 3050011182153. (Corresponding author: Jianjun Ma.)

Guohao Liu, Houjun Sun, and Jianjun Ma are with the Beijing Institute of Technology, Beijing 100081, China, and also with Tangshan Research Institute, BIT, Tangshan 063099, China (e-mail: 3220221571@bit.edu.cn; sunhoujun@bit.edu.cn; jianjun\_ma@bit.edu.cn).

Xiangkun He is with the Department of Bioengineering, Faculty of Engineering, Imperial College London, SW7 2AZ London, U.K. (e-mail: xh1222@ic.ac.uk).

Jiabiao Zhao and Da Li are with the Beijing Institute of Technology, Beijing 100081, China (e-mail: 3120235892@bit.edu.cn; 3220221512@bit.edu.cn).

Hong Liang is with the Meteorological Observation Center of China Meteorological Administration, Beijing 100081, China (e-mail: liangh@cma.gov.cn).

Daniel M. Mittleman is with the School of Engineering, Brown University, Providence, RI 02912 USA (e-mail: daniel\_mittleman@brown.edu).

Color versions of one or more figures in this article are available at <https://doi.org/10.1109/TTHZ.2024.3417319>.

Digital Object Identifier 10.1109/TTHZ.2024.3417319

## I. INTRODUCTION

IN THE dynamic landscape of wireless communications, the exploration of the terahertz (THz) spectrum, encompassing frequencies from 0.1 to 10 THz, has emerged as an essential area in the pursuit of ultrahigh-speed data transmission. This particular segment of the electromagnetic spectrum, notably at its lower frequency range, presents enormous potential for enabling data transmission rates exceeding 100 Gigabits per second (Gbps) [1], [2]. Such groundbreaking capabilities are crucial to meet the burgeoning demands of various data-intensive applications, including, but not limited to, advanced cloud gaming, remote medical procedures like telesurgery, and the ever-evolving realm of the metaverse.

Despite the significant potential of THz frequencies in achieving such remarkable data rates, their practical deployment in wireless systems encounters notable challenges [3], [4], predominantly due to their interaction with atmospheric elements. Contrasting with their behavior in dielectric waveguides [5], [6], THz channel propagation through free space is substantially influenced by gaseous absorption, leading to considerable signal attenuation [7], [8], [9]. This phenomenon, first detailed in ITU-R P.676-10, outlines how water vapor and oxygen contribute to the attenuation of THz frequencies up to 1000 GHz, underpinning much of the current understanding of THz channel dynamics. This attenuation is further intensified in diverse meteorological conditions, including fog, rain, and snow [9], [10], [11], [12], [13], [14], [15], [16]. The recent advancements in THz technology, encompassing developments in both device and radio frequency components, along with innovations in physical layer and medium access control (MAC) layer technologies, have catalyzed a trend of research dedicated to overcoming these propagation challenges. A key strategy in addressing these issues has been the deployment of high-gain directional antennas, which play a critical role in counteracting the intrinsic problems of increased spreading loss and susceptibility to obstructions, a natural characteristic of THz frequencies [17]. However, the incorporation of these advanced technologies introduces extra complexities in MAC protocols and network architecture, necessitating the creation of robust, efficient, and reliable frameworks for communication links.

The effective integration of THz technology into the infrastructure of future wireless communication networks, still needs understanding and overcoming these challenges. Among various atmospheric conditions, snow presents a uniquely complex

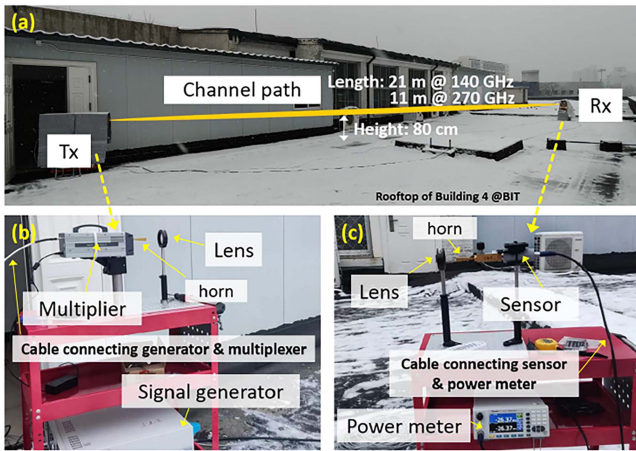


Fig. 1. THz channel measurement setup implemented in the campus of BIT. (a) Outdoor channel on the rooftop of Building 4 at BIT with both transmitter (Tx) and receiver (Rx) safeguarded by waterproof coverings. (b) Transmitter hardware. (c) Receiver hardware.

challenge. The heterogeneous nature and varying densities of snowflakes significantly impact the performance and reliability of THz communication links [18], [19]. The interaction between THz waves and snowflakes results in scattering effects, the full scope and consequences of which are still being extensively explored and remain largely unknown [20], [21]. This gap in knowledge is further highlighted by the complexities involved in accurately measuring and characterizing the impact of snow on THz wave propagation [22].

This work is dedicated to analyze the complexities of THz channel performance in snowy environments. Conducted on the rooftop of Building 4 at Beijing Institute of Technology (BIT), we utilize a comprehensive empirical approach, supported by an array of sophisticated measurement instruments, to thoroughly assess the behavior of THz channels under snowy conditions. This empirical methodology is complemented by theoretical models, offering a holistic and multidimensional view of the dynamics of THz channels in such environments. This extensive investigation is crucial for developing a robust model of THz channels, an integral component in the architecture of future wireless networks, particularly with the advent of the anticipated 6G network paradigm.

## II. CHANNEL MEASUREMENT SETUP

The experimental measurement was conducted in an open-air setting, deploying a fixed point-to-point channel configuration as illustrated in Fig. 1(a). This arrangement required precise positioning of the transmitter and receiver, as depicted in Fig. 1(b) and (c), respectively. For the 140 GHz channel investigation, the components were positioned 21 m apart. In contrast, for the 270 GHz channel, this distance was reduced to 11 m, a modification necessitated by its lower transmit power and the increased path loss characteristic of higher frequency transmission. The rooftop of Building 4 at the BIT was chosen as the experimental site, owing to its conducive environment for atmospheric research.

Central to the transmission system was the Ceyear 1465D signal generator, capable of generating baseband signals in

the range of 100 kHz to 20 GHz. These signals were then up-converted to the targeted THz range (110–170 GHz) using a Ceyear 82406B frequency multiplier module, with a multiplication factor of  $\times 12$ . The continuous wave (CW) signal were radiated through a horn antenna (HD-1400SGAH25), complemented by a dielectric (teflon) lens with a focal length of 10 cm to enhance the signal transmission range. Concurrently, the receiver was equipped with a corresponding and identical horn antenna and lens, directing the incoming signals to a Ceyear 71718 power sensor for direct detection. For the higher frequency range (220–325 GHz), the setup comprised a Ceyear 82406D frequency multiplier (with a multiplication factor of  $\times 18$ ) paired with a Ceyear 89901S horn antenna. The gains of the combination of antennas and lens can be 31 dBi at 140 GHz and 34 dBi at 270 GHz. Both transmission and reception units were elevated 80 cm above the floor, exceeding the radius of the first Fresnel zone (9–11 cm for the 140 GHz channel and 5–6 cm for the 270 GHz channel), and were shielded by a tarp to prevent snow intrusion. The signal beamwidth was measured at  $5.7^\circ$  for 140 GHz, and approximately  $4^\circ$  for 270 GHz. A laptop was employed for control and data acquisition, managing the signal generator and power meter at a data recording frequency of 7 Hz. This equipment setup is in line with previous studies on scattering performance [23], [24] and physical-layer security aspects [25].

To comprehensively assess channel behavior, observations were carried out under two distinct meteorological scenarios: clear weather and snowy conditions. Over a two-day span, data were recorded at 35-s intervals, yielding a substantial dataset representative of each weather scenario. Supplementing this empirical data were atmospheric measurements from the Meteorological Observation Center of the China Meteorological Administration. Data from a meteorological radar situated near the BIT enriched our analysis, providing crucial theoretical insights into link performance amid varying atmospheric dynamics.

## III. ANALYSIS ON CHANNEL POWER PROFILE

Our investigation focused on the efficacy of the outdoor point-to-point THz channel, primarily measured in terms of received power, a critical metric in the design and assessment of wireless communication systems. We concentrated on the 140 GHz and 270 GHz frequencies, where our experimental setup yielded optimal output power. Measurements at 140 GHz were conducted on December 12, 2023, under conditions of approximately  $-1^\circ\text{C}$  temperature and 52% relative humidity (RH), while those at 270 GHz, carried out on December 13, 2023, recorded a marginally lower ambient temperature of  $0^\circ\text{C}$  and higher RH of 60%. These conditions, bordering on the freezing point with elevated humidity, are suggestive of wet snow, a pivotal element in our analysis.

In evaluating THz channel performance under both clear and snowy conditions, we employed the cumulative distribution function (CDF) to scrutinize the power measurements. The data, shown in Fig. 2(a) and (b), were collected at varied intervals, adopting the liquid water equivalent (LWE) precipitation rate as a more precise gauge of snowfall intensity compared to

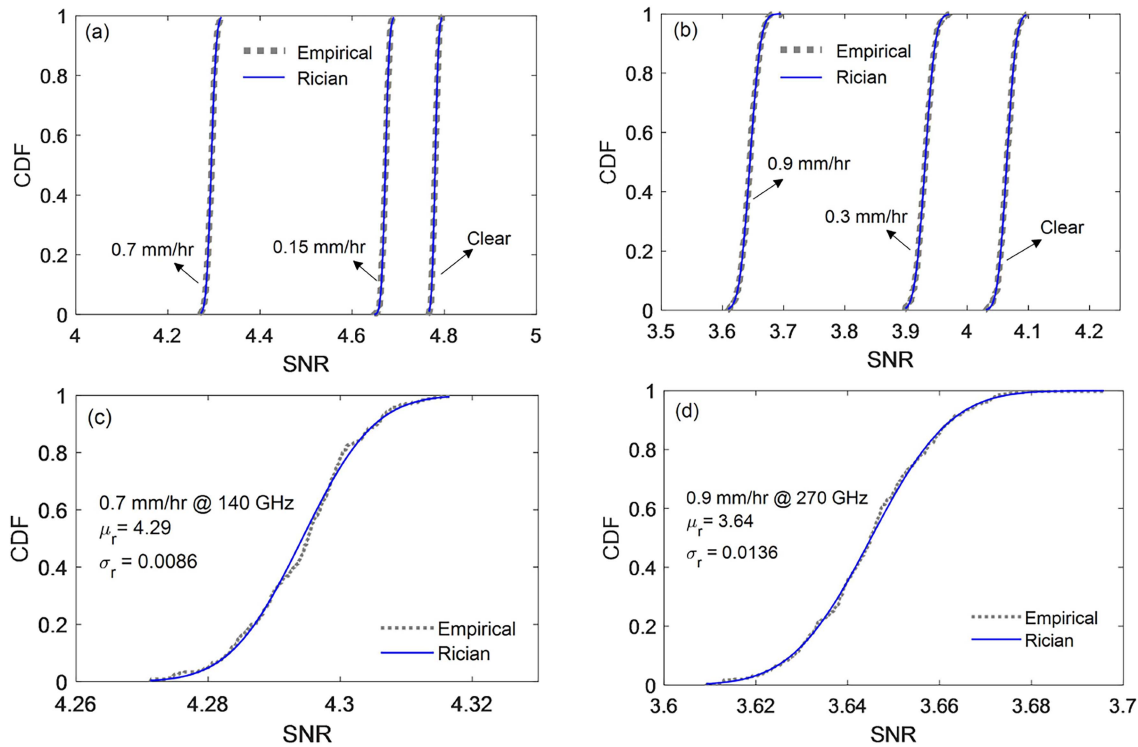


Fig. 2. CDF profile for received SNR with and without snowfall with operating frequencies at (a) 140 and (b) 270 GHz, alongside the fitted CDF to the measured data at (c) 140 and (d) 270 GHz in snowfall conditions.

TABLE I  
PARAMETERS FOR FITTING TO THE RICIAN DISTRIBUTION (PARAMETER  $\mu_r$  REPRESENTS THE MEAN VALUE OF THE RECEIVED POWER LEVEL,  $\sigma_r^2$  DEMOTES THE VARIANCE OF THE RECEIVED SIGNAL'S POWER LEVEL, AND  $K$  SYMBOLIZES THE K-FACTOR FOR THE RICIAN DISTRIBUTION ACROSS DIFFERENT FREQUENCIES AND WEATHER CONDITIONS)

Frequency	Weather condition	$\mu_r$	$\sqrt{\sigma_r^2}$	$K$
140 GHz	Clear	4.78	0.0058	55.3 dB
	Snowy (0.15 mm/hr)	4.67	0.0070	53.4 dB
	Snowy (0.7 mm/hr)	4.29	0.0086	51 dB
270 GHz	Clear	4.06	0.0118	47.7 dB
	Snowy (0.3 mm/hr)	3.93	0.0130	46.6 dB
	Snowy (0.9 mm/hr)	3.64	0.0136	45.6 dB

traditional visibility metrics. This methodology, informed by the diversity in snow types and their distinct impacts on visibility [26], is in line with the LWE intensity guidelines set forth by the SAE Ground Deicing Committee in 1988 [27]. The signal-to-noise (SNR) ratio was obtained by subtracting the noise from the received power. The noise measurements obtained through our power meter inherently include system noise, comprising both the external noise from the environment and the internal noise generated by our measurement apparatus. Our results, detailed in Table I, indicate a discernible trend of power reduction across both the 140 GHz and 270 GHz channels as LWE rates

increasing, hinting that extended transmission distances may amplify this loss. This observation underscores the potential necessity for counteracting methodologies and techniques in THz wireless communication systems to counteract the effects of various atmospheric conditions.

A comparison of the CDF curves in clear versus snowy conditions revealed no substantial difference as in Fig. 2, implying minimal scattering effects from snowfall. This was substantiated by fitting the CDF data to a Rician distribution model, as illustrated in Table I. The correspondence of the CDF with a Rician distribution in both conditions, as opposed to the expected Weibull distribution [21], marks a notable deviation. We attribute this to atmospheric turbulence [22] and its influence on pointing errors. It is noteworthy that wind speeds during our measurements were relatively mild, below 5 m/s (light breeze), thus unlikely to induce significant turbulence-induced pointing errors, especially for THz frequency band [8].

K factor refers to the ratio of the power of the line-of-sight (LoS) path signal to the power of the reflected or scattered signals (multipath components). The observed high K factor in snowy conditions, as shown in Table I, suggests a dominant LoS component. This leads us to infer that multipath effects, typically a result of scattering, are minimal in our measurement scenario again, aligning with findings in rainy conditions [28]. This is further supported by the observation that the presence of snowflakes did not significantly contribute to multipath components, consistent with prior studies on multipath profiles [18]. Additionally, the increased propagation loss due to the elongated path length of multipath components, relative to the LoS path, also supports this conclusion.



Nevertheless, this does not invalidate the impact of snow on the channel's phase performance. The variability in signal strength, indicated by the variance  $\sigma_r^2$  in the received signal's SNR, is ascribed to dynamic interactions with moving snowflakes. These interactions result in signal strength fluctuations and illuminate the multiplicative nature of signal degradation over distance, a phenomenon also noted in rainy conditions [11], [29]. In this work, it is crucial to account for the statistical distribution of signal variability along with time-variant channel characteristics, such as rapid phase and amplitude changes. Although we emphasize the need to consider time-variant LWE precipitation rates to fully capture these rapid fluctuations, the limitations in meteorological data acquisition, typically performed at hourly intervals, restrict our ability to thoroughly characterize these fast fluctuations (scintillation effects) observed in atmospheric turbulence measurements [8]. Furthermore, temporal variations in snowfall density and distribution could impact the consistency of signal reception. Nonetheless, our measurement protocol, with a recording interval of 1/7 s, exceeds the transient period (approximately 0.03 s) required for a wet snowflake, moving at an average speed of 1.5 m/s [19], to cross the beam width of roughly 5 cm in diameter, posing a challenge in distinctly identifying and analyzing these rapid fluctuations.

#### IV. ANALYSIS ON CHANNEL POWER LOSS

In this section, we explore the intricate dynamics of snow and its impact on THz channel propagation, with a specific focus on power loss. To effectively quantify the power loss attributable to snow, it is imperative to monitor the temporal variations and aggregate these data to deduce average values and corresponding uncertainties. As demonstrated in Fig. 3, the measured data unambiguously indicate a progressive increase in power loss correlating with rising snowfall rates, corroborating trends identified in previous studies [20]. However, the challenge lies in accurately modeling these fluctuations, given the diverse forms and distribution of snowflakes, as stated above.

In the analytical approach, we have employed several theoretical models, including ITU-R P.1817-1 [30], the Gunn-East model based on the Rayleigh approximation [31], and the renowned Mie scattering theory [32], in conjunction with the Scott distribution for snowflakes [33]. These models provide a nuanced understanding of the impact of snow on THz signal propagation. The Scott distribution, expressed as a negative exponential function  $N(r) = N_0 \exp(-\Lambda r)$ , with parameters  $N_0 = 100 \times 10^3$  and  $\Lambda = 5.76R^{-0.31}$ , is proved particularly useful in our calculations, offering a more refined analysis compared to other distributions, like Marshall–Palmer, Gunn–Marshall, and Sekhon–Srivastava [20]. The Mie scattering theory model employs the dielectric properties of snow using Debye's mixture theory [19], [34], by using the double-Debye dielectric model (D3M) [35] for water and a single Debye model for ice [36], [37]. It assumes the snowflakes as spherical particles, which may not accurately represent the complex shapes and fractal nature of snowflakes. Additionally, gaseous absorption along the channel

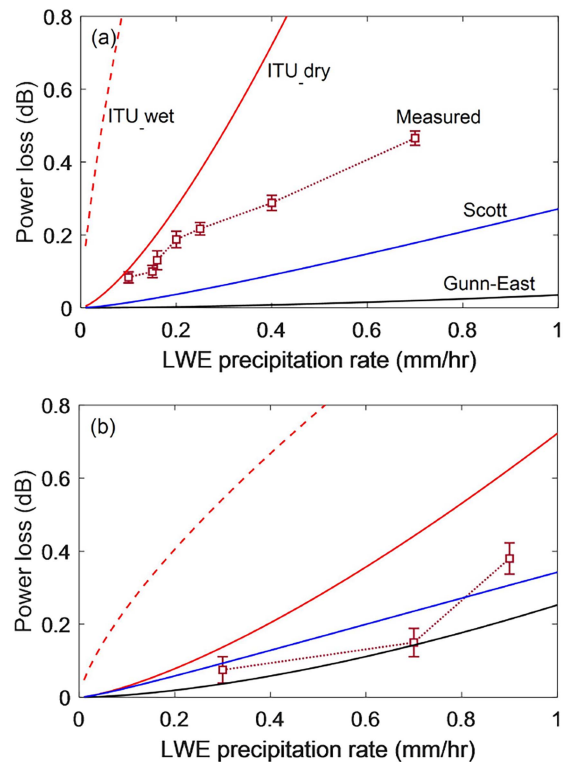


Fig. 3. Power loss relative to the LWE precipitation rate for the 140 and 270 GHz channels, over distances of 21 and 11 m, respectively. (b) Keeps an identical legend and marks as (a).

path was accounted for using the ITU-R recommendation model [38], validated for frequencies between 1 and 450 GHz [39].

Our theoretical prediction, as depicted in Fig. 3(a) and (b), reveals that while the ITU model tends to overestimate power loss, the Gunn–East model, more apt for millimeter-wave channels below 70 GHz, significantly underestimates it. The Mie scattering theory (called the Scott model in the following parts), given the size of snow particles relative to THz wavelengths [40], provides a closer approximation, albeit with occasional underestimations as evidenced in previous findings [20]. The empirical data reside between the predictions of the Scott and ITU models, suggesting that a combined approach integrating both models could yield more accurate predictions. For our computations, wet snow parameters were considered, in line with the near-freezing temperatures and high humidity during our measurements. Interestingly, the ITU model for dry snow more closely matched our empirical data than that for wet snow, prompting its inclusion in the following analyses. The estimated wetness ( $m_v$ ) of the snowflakes, assumed to be 10%, was not empirically measured but estimated.

Addressing the complexities of accurately modeling channel power attenuation due to snowfall, we also considered empirical fitting, as suggested in ITU-R Recommendation. This method, defined by the following:

$$\gamma_{\text{snow}} = a \cdot \text{Rr}^b [\text{dB/km}] \quad (1)$$

where  $a$  and  $b$  are empirically derived constants, and  $\text{Rr}$  refers the LWE rate of precipitation in mm/hr, offers a practical approach

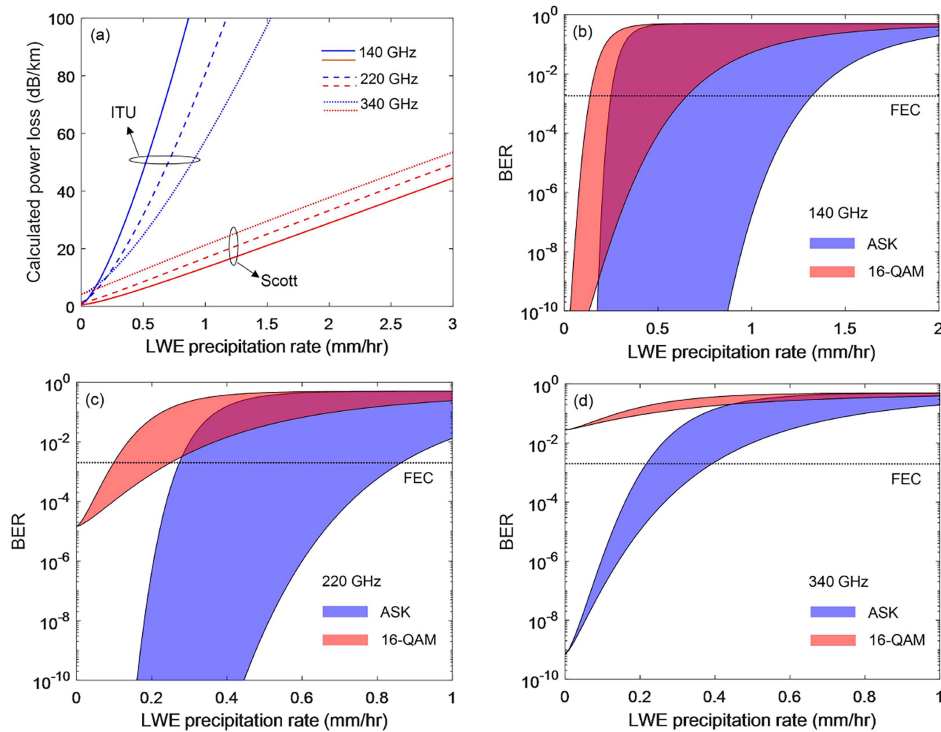


Fig. 4. (a) Calculated average power loss with respect to LWE rate suffered by channels operating at 140, 220, and 340 GHz. Predicted average BER performance of the channels operating at (b) 140 GHz, (c) 220 GHz, and (d) 340 GHz. The upper and lower bounds of the predicting area correspond to the predictions by ITU model (dry) and Scott model, respectively. Channel distance 1 km, relative humidity RH 60%, temperature 0 °C, transmitted power 20 dBm, noise level of receiver -60 dBm; the gain at the transmitter and receiver side is identical and equals to 40 dB (combination of antenna and lens).

for aligning the model with observed data. For this, we obtained constants  $a = 29.79$ ,  $b = 0.82$  for 140 GHz and  $a = 30.28$ ,  $b = 1.15$  for 270 GHz by a power-fitting algorithm. This technique is advantageous in scenarios where theoretical models are insufficient to capture the intricate interactions between THz frequencies and snow particles. However, this specific attenuation model may not be universally applicable across varied environmental conditions or geographical locations, as it is typically tailored to specific datasets or conditions. Another limitation is its reliance on the availability and quality of measured data, without providing deeper theoretical insights. Consequently, we intend to continue employing the Scott model for further theoretical investigations.

## V. THEORETICAL ANALYSIS ON CHANNEL PERFORMANCE

The preceding theoretical model illuminates signal attenuation and power profile in THz channels. However, translating these findings into a comprehensive understanding of communication link reliability requires a deeper exploration. To this end, bit-error-ratio (BER) analysis becomes an indispensable tool, offering critical insights into how power variations influence the error rates in transmitted data. Such an analysis is not only fundamental for evaluating the channel's efficacy but also necessary for designing and optimizing wireless communication systems in the THz band, where atmospheric elements like humidity, precipitation, and temperature profoundly affect signal transmission. By dissecting the impact of these atmospheric factors on BER, it is helpful to refine antenna design, signal processing

algorithms, and error correction techniques to reinforce the system's overall performance and reliability.

In this section, we conduct a detailed theoretical examination of channel performance under diverse LWE precipitation rates. As depicted in Fig. 4(a), an obvious observation emerges: the discrepancy between the ITU and Scott model predictions becomes smaller as the carrier frequency increases, suggesting a heightened consistency and reliability of both models at higher frequency bands. Notably, the Scott model, corroborated by previous research [17], more accurately forecasts an increased power loss at higher frequencies. Concurrently, the ITU model exhibits improved accuracy as the carrier frequency nears the upper band, showing closer alignment with the optical frequency range.

Our efforts focus then shifts to the BER performance of various channels under clear and snowy conditions, applying an LWE precipitation rate of 1 mm/hr. The selected modulation schemes for this analysis are amplitude shift keying (ASK) and 16-quadrature amplitude modulation (16-QAM), chosen based on their deployment in our prior studies [11], [19], [29]. ASK's sensitivity to amplitude fluctuations makes it particularly suitable for assessing the influence of varying atmospheric conditions. Conversely, QAM, utilizing both amplitude and phase changes for data transmission, offers a more comprehensive evaluation of signal integrity under different weather scenarios. The BER performance is predicted using established mathematical expressions

$$\text{BER}_{\text{ASK}} = Q\left(\sqrt{2 \cdot \text{SNR}}\right) \quad (2)$$

and

$$\text{BER}_{16\text{-QAM}} = \frac{4}{\sqrt{M}} \cdot Q\left(\sqrt{\frac{3 \cdot \text{SNR}}{M-1}}\right) \quad (3)$$

incorporating the  $Q$ -function to denote the probability of a Gaussian random variable exceeding a specified value, with modulation order denoted by  $M$ . The operational frequencies under consideration—140, 220, and 340 GHz—fall within atmospheric transparency windows and are commonly used in various wireless link configurations [41].

A predictable finding is that lower carrier frequencies and simpler modulation orders, such as ASK, lead to improved BER performance. This enhancement at lower frequencies is ascribed to the greater power loss typically observed at higher frequencies. Moreover, advanced modulation schemes necessitate a higher SNR for equivalent BER values, rendering them more prone to errors in snowy conditions. It is noteworthy that under specific conditions, error-free data transmission ( $\text{BER} < 10^{-10}$ ) is feasible, particularly at lower frequencies and with simpler modulation techniques. This underscores the strategic selection of frequency and modulation strategy for THz communications in challenging atmospheric scenarios.

Optimal THz channel performance is observed with LWE precipitation rates below 1 mm/hr, typically associated with light snowfall conditions [27]. This finding indicates that light snowfall exerts minimal impact on THz communication over distances of up to 1 km. Nevertheless, the reliability of the channel decreases with either an increase in distance or snowfall intensity. Incorporating forward error correction (FEC) could enhance error resilience by correcting errors within its threshold (typically  $2 \times 10^{-3}$ ), although its effectiveness is bounded by the complexity of the coding scheme and the level of redundancy introduced.

To broaden our understanding of channel performance in relation to operating frequency, we conducted an extensive analysis encompassing power loss and BER evolution. This analysis, accounting for atmospheric absorption factors such as 60% RH and a temperature of 0 °C, utilized the Scott model. Setting the LWE precipitation rate at 0.5 mm/hr and maintaining the channel distance at 1 km, we observed in Fig. 5(a) that lower frequencies exhibit reduced sensitivity to changes in humidity. Under ASK modulation, the operational frequency can reach up to 420 GHz in clear conditions, while it is limited to 260 GHz under 16-QAM in similar conditions. However, in snowy scenarios, the threshold frequency drops to 260 GHz for ASK and 140 GHz for 16-QAM, considering the FEC threshold. Notably, variations in atmospheric humidity also influence the wetness of snowflakes, a factor not accounted for in this theoretical model due to the complex mechanisms underlying this interaction.

As ambient temperature increases, the air's capacity to retain water vapor (saturation vapor density) also rises. Consequently, if vapor density remains constant while temperature escalates, relative humidity decreases due to the air's enhanced capacity to hold more water vapor [42]. In the context of THz communications, especially under conditions of wet snowfall (temperatures ranging from 0 °C to 3 °C), understanding the interplay between

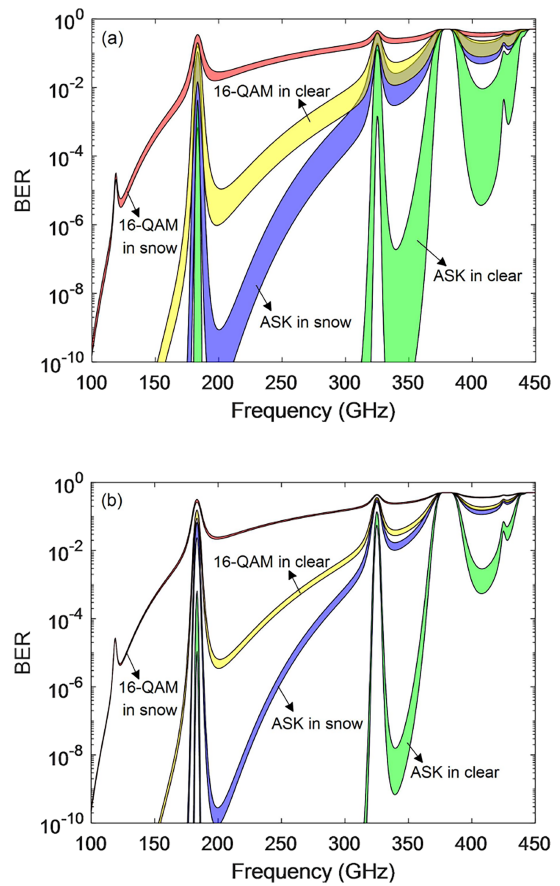


Fig. 5. Calculated average BER performance due to the variation of (a) relative humidity and (b) ambient temperature. Channel distance 1 km, humidity RH 60%, temperature 0 °C, transmitted power 20 dBm, noise level of receiver -60 dBm, LWE rate 0.5 mm/hr; the gain at the transmitter and receiver side are identical and equals to 40 dB (combination of antenna and lens).

atmospheric conditions and THz wave propagation is crucial. Our findings in Fig. 5(b) suggest that within this specific temperature range, temperature variations have negligible influence on THz frequency propagation below 200 GHz. This implies that despite potential changes in temperature affecting relative humidity, the propagation characteristics of THz channel within this frequency band largely remain stable, a critical factor for ensuring consistent communication quality and reliability in regions experiencing wet snowfall.

## VI. CONCLUSION

In this work, we conducted a comprehensive investigation on THz channel performance under snowy conditions, utilizing a combination of outdoor measurements and advanced channel modeling techniques. A specialized measurement setup was established at the BIT, facilitating an in-depth analysis on the power profile, link budget, and BER performance in snowy weather conditions. Our findings were particularly revealing in the context of CDF profiles under both clear and snowy conditions. These profiles consistently conformed to Rician distributions with variable K-factors, an observation pointing



towards the minimal impact of multipath effects in our experimental setup. Additionally, our study highlighted the rapid power fluctuations induced by the dynamic interaction between THz waves and moving snowflakes.

In the realm of theoretical modeling, the Scott model emerged as a more accurate predictor. Employing it for BER predictions revealed that lower carrier frequencies and simpler modulation orders, lead to improved BER performance, even though light snowfall can significantly impact BER performance. This work also delved into the influence of ambient humidity and temperature on THz communication, finding that lower frequencies are less susceptible to humidity variations and that within a specific temperature range, the impact of temperature changes on THz frequency propagation below 200 GHz is negligible.

Despite these contributions, this work faced certain limitations. The current experimental setup's inability to accurately capture rapid power fluctuations limited our investigation into scintillation effects, an area we aim to focus on in the future. Additionally, we hypothesize that snowflakes, when moving at sufficient velocities, might induce a Doppler shift in the received THz signal, potentially affecting the signal's phase. This phenomenon is likely to be more pronounced at higher transmission frequencies and thus merits further investigation.

#### REFERENCES

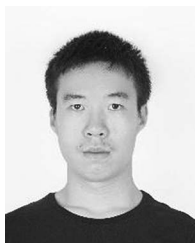
- [1] T. Kürner, D. M. Mittleman, and T. Nagatsuma, *THz Communications: Paving the Way Towards Wireless Tbps*. Cham, Switzerland: Springer, 2021.
- [2] K. Guan, H. Yi, D. He, B. Ai, and Z. Zhong, "Towards 6G: Paradigm of realistic Terahertz Channel modeling," *China Commun.*, vol. 18, no. 5, pp. 1–18, 2021.
- [3] X. Cai, X. Cheng, and F. Tufvesson, "Toward 6G with terahertz communications: Understanding the propagation channels," *IEEE Commun. Mag.*, vol. 62, no. 2, pp. 32–38, Feb. 2024.
- [4] K. Guan, H. Yi, D. He, and Z. Lai, "Chapter 19: Terahertz communications on various beyond 5G real-world use cases for IoT, railway, train, drone communications - propagation channel characterization and challenges," *Metrol. 5G Emerg. Wireless Technol., Inst. Eng. Technol.*, 2021, ISBN 978-1-83953-278-8.
- [5] G. Liu et al., "Myelin sheath as a dielectric waveguide for signal propagation in the mid-infrared to terahertz spectral range," *Adv. Funct. Mater.*, vol. 29, 2019, Art. no. 1807862.
- [6] J. Ma, M. Weidenbach, R. Guo, M. Koch, and D. M. Mittleman, "Communications with THz waves: Switching data between two waveguides," *J. Infrared, Millimeter, Terahertz Waves*, vol. 38, no. 11, pp. 1316–1320, 2017.
- [7] Y. Yang, M. Mandehgar, and D. R. Grischkowsky, "Understanding THz pulse propagation in the atmosphere," *IEEE Trans. Terahertz Sci. Technol.*, vol. 2, no. 4, pp. 406–415, Jul. 2012.
- [8] J. Ma, L. Moeller, and J. F. Federici, "Experimental comparison of terahertz and infrared signaling in controlled atmospheric turbulence," *J. Infrared, Millimeter Terahertz Waves*, vol. 36, no. 2, pp. 130–143, 2015.
- [9] J. Ma, R. Shrestha, L. Moeller, and D. M. Mittleman, "Invited article: Channel performance for indoor and outdoor terahertz wireless links," *APL Photon.*, vol. 3, no. 5, 2018, Art. no. 051601.
- [10] Y. Yang, M. Mandehgar, and D. R. Grischkowsky, "Broadband THz signals propagate through dense fog," *IEEE Photon. Technol. Lett.*, vol. 27, no. 4, pp. 383–386, Feb. 2015.
- [11] J. Ma, F. Vorrius, L. Lamb, L. Moeller, and J. F. Federici, "Experimental comparison of terahertz and infrared signaling in laboratory-controlled rain," *J. Infrared, Millimeter Terahertz Waves*, vol. 36, no. 9, pp. 856–865, 2015.
- [12] K. Su, L. Moeller, R. B. Barat, and J. F. Federici, "Experimental comparison of terahertz and infrared data signal attenuation in dust clouds," *J. Opt. Soc. Am. A*, vol. 29, no. 11, pp. 2360–2366, 2012.
- [13] K. Su, L. Moeller, R. B. Barat, and J. F. Federici, "Experimental comparison of performance degradation from terahertz and infrared wireless links in fog," *J. Opt. Soc. Am. A*, vol. 29, no. 2, pp. 179–184, 2012.
- [14] Q. Jing, D. Liu, and J. Tong, "Study on the scattering effect of terahertz waves in near-surface atmosphere," *IEEE Access*, vol. 6, pp. 49007–49018, 2018.
- [15] G. A. Siles, J. M. Riera, and P. Garcia-del-Pino, "Atmospheric attenuation in wireless communication systems at millimeter and THz frequencies," *IEEE Antennas Propag. Mag.*, vol. 57, no. 1, pp. 48–61, Feb. 2015.
- [16] E.-B. Moon, T.-I. Jeon, and D. R. Grischkowsky, "Long-path THz-TDS atmospheric measurements between buildings," *IEEE Trans. Terahertz Sci. Technol.*, vol. 5, no. 5, pp. 742–750, Sep. 2015.
- [17] G. B. Wu, Y.-S. Zeng, K. F. Chan, S.-W. Qu, and C. H. Chan, "High-gain circularly polarized lens antenna for terahertz applications," *IEEE Antennas Wireless Propag. Lett.*, vol. 18, no. 5, pp. 921–925, May 2019.
- [18] P. Sen et al., "Terahertz communications can work in rain and snow: Impact of adverse weather conditions on channels at 140 GHz," in *Proc. 6th ACM Workshop Millimeter-Wave Terahertz Netw. Sens. Syst.*, 2022, pp. 13–18.
- [19] J. Ma, J. Adelberg, R. Shrestha, L. Moeller, and D. M. Mittleman, "The effect of snow on a terahertz wireless data link," *J. Infrared, Millimeter Terahertz Waves*, vol. 39, no. 6, pp. 505–508, 2018.
- [20] Y. Amarasinghe, W. Zhang, R. Zhang, D. M. Mittleman, and J. Ma, "Scattering of terahertz waves by snow," *J. Infrared, Millimeter, Terahertz Waves*, vol. 41, pp. 215–224, 2019.
- [21] M. Taherkhani, Z. G. Kashani, and R. Sadeghzadeh, "Average bit error rate and channel capacity of terahertz wireless line-of-sight links with pointing errors under combined effects of turbulence and snow," *Appl Opt.*, vol. 59, no. 33, 2020, Art. no. 10345.
- [22] M. Taherkhani, Z. G. Kashani, and R. A. Sadeghzadeh, "On the performance of THz wireless LOS links through random turbulence channels," *Nano Commun. Netw.*, vol. 23, 2020, Art. no. 100282.
- [23] P. Li et al., "Scattering and eavesdropping in terahertz wireless link by wavy surfaces," *IEEE Trans. Antennas Propag.*, vol. 71, no. 4, pp. 3590–3597, Apr. 2023.
- [24] J. Liu et al., "High-speed surface roughness recognition by scattering on terahertz waves," in *Proc. 16th U.K.-Europe-China Workshop Millimeter Waves Terahertz Technol.*, Guangzhou, China, 2023, vol. 1, pp. 1–3.
- [25] Y. Qiao et al., "Tubular eavesdropper on a terahertz link - A tentative study," in *Proc. 16th U.K.-Europe-China Workshop Millimeter Waves Terahertz Technol.*, Guangzhou, China, 2023, vol. 1, pp. 1–2.
- [26] R. M. Rasmussen, J. Vivekanandan, J. Cole, B. Myers, and C. Masters, "The estimation of snowfall rate using visibility," *J. Appl. Meteorol.*, vol. 38, no. 10, pp. 1542–1563, 1998.
- [27] T. Fahey, "Snowfall rate thresholds for light, moderate and heavy," in *Proc. Aerodrome Meteorological Observ. Forecast Study Group, 7th Meeting*, Montréal, Canada, Sep. 9–12, 2008.
- [28] R. Wang, Y. Mei, X. Meng, and J. Ma, "Secrecy performance of terahertz wireless links in rain and snow," *Nano Commun. Netw.*, vol. 28, 2021, Art. no. 100350, doi: 10.1016/j.nancom.2021.100350.
- [29] P. Li et al., "Performance degradation of terahertz channels in emulated rain," *Nano Commun. Netw.*, vol. 35, 2023, Art. no. 100431.
- [30] "International Telecommunication Union Recommendation ITU-R P.1817-1: Propagation data required for the design of terrestrial free-space optical links," 2012. [Online]. Available: <https://www.itu.int/rec/R-REC-P.676-13-202208-I/en>
- [31] K. L. S. GUM and T. W. R. East, "The microwave properties of precipitation particles," *Quart. J. Roy. Meteorological Soc.*, vol. 80, no. 346, pp. 522–545, 1954.
- [32] D. Deirmendjian, *Electromagnetic Scattering On Spherical Polydispersions*. New York, NY, USA: American Elsevier Publishing, 1969.
- [33] B. C. Scott, "Theoretical estimates of the scavenging coefficient for soluble aerosol particles as a function of precipitation type, rate and altitude," *Atmospheric Environ.*, vol. 16, no. 7, pp. 1753–1762, 1982.
- [34] J. E. Justo, "Types of snowfall," vol. 54, no. 11, pp. 1148–1162, 1973.
- [35] F. T. Ulaby, R. K. Moore, and A. K. Fung., *Microwave Remote Sensing: Active and Passive. Volume II-Radar Remote Sensing and Surface Scattering and Emission Theory*. Norwood, MA, USA: Artech House, 1982.
- [36] O. Mishima, D. D. Klug, and E. Whalley, "The far-infrared spectrum of ice in the range 8–25 cm<sup>-1</sup>. Sound waves and difference bands, with application to Saturn's rings," *J. Chem. Phys.*, vol. 78, no. 11, pp. 6399–6404, 1983.
- [37] J. H. Jiang and D. L. Wu, "Ice and water permittivities for millimeter and sub-millimeter remote sensing applications," *Atmospheric Sci. Lett.*, vol. 5, no. 7, pp. 146–151, 2004.

- [38] "International Telecommunication Union Recommendation (ITU-R) P.676-13: Attenuation by atmospheric gases and related effects." [Online]. Available: <https://www.itu.int/rec/R-REC-P.676-13-202208-I/en>
- [39] J. F. Ohara and D. R. Grischkowsky, "Comment on the veracity of the ITU-R recommendation for atmospheric attenuation at terahertz frequencies," *IEEE Trans. Terahertz Sci. Technol.*, vol. 8, no. 3, pp. 372–375, May 2018.
- [40] H. R. Pruppacher and J. D. Klett, *Microphysics of Clouds and Precipitation*. Norwell, MA, USA: Kluwer, 1997.
- [41] T. Nagatsuma, G. Ducournau, and C. C. Renaud, "Advances in terahertz communications accelerated by photonics," *Nature Photon.*, vol. 10, no. 6, pp. 371–379, 2016.
- [42] C. D. Ahrens, *Meteorology Today: An Introduction to Weather, Climate, and the Environment*. VA, USA: Thomson/Brooks/Cole, 2003.



**Guohao Liu** received the graduation degree in electronic information from Nanjing Normal University, Nanjing, China, in 2022. He is currently working toward the master's degree in electronic information technology with the Institute of Microwave and Terahertz, School of Integrated Circuits and Electronics, Beijing Institute of Technology, Beijing, China.

His research interest includes grain moisture detection.



**Xiangkun He** received the B.Sc. degree in electronic engineering from the University of Central Lancashire, Preston, U.K., in 2021, and the M.Sc. degree in electric and electronic engineering from the University of Sheffield, Sheffield, U.K., in 2022. He is currently working toward the M.Sc. degree in biomedical engineering with the Imperial College London, London, U.K.



**Jiabiao Zhao** received the bachelor's degree in communication engineering from Zhengzhou University, Henan, China, in 2021. He is currently working toward the doctor's degree with the School of Integrated Circuits and Electronic, Beijing Institute of Technology, Beijing, China.

His main research interests include meteorological radar and radar calibration techniques in different weather conditions.



**Da Li** received the bachelor's degree in communication engineering from Shandong University, Jinan, China, in 2022.

He is currently with the School of Integrated Circuits and Electronics, Beijing Institute of Technology, Beijing, China, majoring in New-Generation Electronic Information Technology. His research interest includes terahertz channel model.



**Hong Liang** received the Ph.D. degree in atmospheric science from the University of Chinese Academy of Sciences, Beijing, China, in 2012.

From 2017 to 2018, he was a Visiting Scholar with the Scripps Institution of Oceanography, University of California San Diego, La Jolla, CA, USA. He has been working as a Researcher with the Meteorological Observation Center, China Meteorological Administration, Beijing China. His recent research interests include GNSS-refractometry remote sensing and GNSS-reflectometry remote sensing.



**Houjun Sun** received the B.S. degree in engineering, the M.S. degree in electromagnetic field and microwave technology, and the Ph.D. degree in communication and electronic systems from the Department of Electronic Engineering, the Beijing Institute of Technology, Beijing, China, in 1991, 1994, and 1997, respectively.

After that, he worked with the Beijing Institute of Technology. He is currently a Full Professor with the Beijing Key Laboratory of Millimeter and Terahertz Wave Technology and the School of Integrated circuits and Electronic.

His current research interests include millimeter/terahertz antennas and integrated chips.



**Daniel M. Mittleman** (Fellow, IEEE) received the B.S. degree from the Massachusetts Institute of Technology, Cambridge, MA, USA, in 1988, and the M.S. and Ph.D. degrees from the University of California, Berkeley, Berkeley, CA, USA, in 1990 and 1994, respectively, under the direction of Dr. Charles Shank, all in physics.

He then joined AT&T Bell Laboratories as a Postdoctoral member of the technical staff, working first for Dr. Richard Freeman on a terawatt laser system, and then for Dr. Martin Nuss on terahertz spectroscopy and imaging. He joined the ECE Department, Rice University in 1996. In 2015, he moved to the School of Engineering, Brown University, Providence, RI, USA. His research interests include the science and technology of terahertz radiation.

He is a Fellow of the OSA and the APS. He was the recipient of the Humboldt Research Award in 2018. During 2018–2020, he served a three-year term as Chair of the International Society for Infrared Millimeter and Terahertz Waves, and received the Society's Exceptional Service Award in 2022. In 2023–2025, he is a Mercator Fellow of the Deutsche Forschungsgemeinschaft (DFG), in affiliation with the Meteracom project.



**Jianjun Ma** (Member, IEEE) was born in Qingdao, China, in 1986. He received the Ph.D. degree in applied physics from New Jersey Institute of Technology, Newark, NJ, USA, in 2015, under the guidance of Prof. John F. Federici. His Ph.D. dissertation was about the weather impacts on outdoor terahertz and infrared wireless communication links.

In 2016, he joined Prof. Daniel M. Mittleman's Group, Brown University, Providence, RI, USA, as a Postdoctoral Research Associate. In 2019, he joined the Beijing Institute of Technology, Beijing, China, as a Professor. His current research interests include terahertz communication and sensing, indoor/outdoor wireless channel measurement and modeling.